

Heteronuclear Bimetallic Organic Molecular Enabling Targeted Synthesis of Efficient Pt1Fe1 Intermetallic Compound for Oxygen Reduction Reaction

Dechao Lai^{ab}, Qingqing Cheng^{a*}, Yu Zheng^{ab}, Hao Zhao^{ab}, Yubin Chen^{ab}, Weibo Hu^a, Zhiqing Zou^a, Ke Wen^a, Liangliang Zou^{a*} and Hui Yang^{a*}

a. Shanghai Advanced Research Institute, Chinese Academy of Sciences, Shanghai 201210, China, chengqq@sari.ac.cn; zoull@sari.ac.cn and yangh@sari.ac.cn

b. University of Chinese Academy of Sciences, Beijing 100049, China

Experimental Procedures

1.1 Materials:

All reagents are not purified. Therein, trans-Diiodobis(triethylphosphine)platinum (trans-PtI₂(PEt₃)₂) was synthesized based on the literature¹. Ethynylferrocene (C₁₂H₁₀Fe) was purchased from Shanghai Haohong scientific Co., Ltd. Copper(I) Iodide, diethylamine were obtained from Shanghai Titan Technology Co., Ltd.

1.2. Synthesis of Heteronuclear Bimetallic Organic Molecular (HBOM):

2.766 g trans-PtI₂(PEt₃)₂ and 636.3 mg C₁₂H₁₀Fe were added to a 250 ml double-neck round-bottom flask. A rubber sieve and a tee connection with a nitrogen balloon were adopted to seal the double-neck round-bottom flask without air. Then 50 ml of toluene and 34 ml of diethylamine were added to the flask via syringe. The reaction solution was stirred at room temperature for 15 min until the solid was almost dissolved. Dispersed 67 mg CuI into 10 ml toluene solution and added it to the reaction solution by syringe in batches. After the reaction solution was stirred for two days, sufficient silica gel was added and the solvent was removed in vacuo. The HBOM was obtained by column chromatography with a solvent mixture (Dichloromethane /Petroleum Ether :1/1). Yield: 1.80 g, 78%. ¹H NMR (CDCl₃): δ 1.187 (m 18H), δ 2.225 (m 12H), δ 4.079 (s 2H), δ 4.140 (s 5H), δ 4.233 (s 2H).

1.3. Preparation of catalyst:

Added 100 mg HBOM and 40 mg Vulcan XC-72 carbon power to a 100 ml beaker with 40 ml tert-butanol and ultrasonically dispersed the solution for 1 h. Then the solution was freeze-dried to obtain a black powder that was uniformly mixed with HBOM and Vulcan XC-72. High temperature tube furnace was used to heat treat the precursors. PtFe intermetallic compound was obtained by thermal treatment at 700 °C under NH₃ for 2 h with 10 °C min⁻¹ heating rate. Subsequently, PtFe catalysts were washed by 0.5 M H₂SO₄ at 60 °C for 0.5 h. Finally, the catalyst after being washed in deionized water and dried was denoted as Pt1Fe1-IMC/C.

Disordered alloy was synthesized by the same method except that it was treated at 600 °C for 3 h. Then it was denoted as D-PtFe/C. To explore the evolution of PtFe alloys and particle size, some samples were prepared under the same conditions as Pt1Fe1-IMC/C except for different heat treatment time and temperature were denoted as 200, 300, 400, 500, 600, 700, 700-1h, 700-2h, 800, 900 respectively.

Preparation of PtFe catalyst by coprecipitation: 2.59 ml of K₂PtCl₄ solution (10 mg/ml), 270.3 μL of FeCl₃ solution (50 mg/ml), 50 mg Vulcan XC-72 carbon power and 17 ml of deionized water were added into 100 ml beaker with an ultrasonic dispersion for 1h. Then, the solution was freeze-dried to obtain a black solid powder. Subsequently, black powder was heated treat at 700 °C under NH₃ for 2 h with 10 °C min⁻¹ heating rate. Finally, the catalyst was etched by 0.5M H₂SO₄ in 60 °C for 0.5h, followed by washing with deionized water. Then it was denoted as PtFe/C-P.

2. Physical characterization:

A Bruker D8 Advanced XRD, with Cu K α 1 radiation ($\lambda = 0.15$ nm) which the tube voltage was maintained at 40 KV and 20 mA was conducted to obtain the XRD pattern results. The metal loading of the PtFe catalysts were detected by inductively coupled plasma atomic emission spectroscopy (ICP-AES, Thermo America). X-ray photoelectron spectroscopy (XPS) (Kratos Axis Ultra^{DL}, Britain) with Al K α radiation was employed to measure the chemical state of catalysts. Meantime, X-ray adsorption spectroscopies obtained at the beamline BL08U1-A of Shanghai Synchrotron Radiation Facility. Finally, JEOL JEM-2100F TEM and Aberration-Corrected TEM with a Probe Corrector equipped for HAADF images and elemental mapping were carried out to investigate the morphology of the catalysts, which the sample were prepared at copper grid.

3. Electrochemical characterization

All electrochemical tests adopted a three-electrode system. Therein, the counter electrode was platinum wire, the reference electrode was Hg/Hg₂SO₄ and work electrode was a glassy carbon electrode with an area of 0.196 cm². CHI730E Potentiostat/ Galvanostat was employed to control the current and voltage. Firstly, 4 mg of catalyst was dispersed in 2 ml of mixed solvent (deionized water: isopropyl alcohol: 5 wt.% Nafion = 0.96: 1: 0.04) to obtain the uniform ink. Then, 7 μ L ink was dropped into RDE and dried under incandescent light bake. Subsequently, 200 cyclic voltammetry loops were carried out to activate the catalyst at 0.05- 1.5 V (vs. RHE) potential with a sweep rate of 100 mV s⁻¹, which the electrolyte was 0.1M N₂-saturated HClO₄ at room temperature.

CV curves were obtained at 0.05- 1.1 V (vs. RHE) with a sweep rate of 50 mV s⁻¹ in a 0.1M N₂-saturated HClO₄ solution. Meantime, the linear sweep voltammetry (LSV) curves at 0.05-1.1 V (vs. RHE) potential with a sweep rate of 10 mV s⁻¹ were employed to describe the activity of catalysts in a 0.1M O₂-saturated HClO₄ solution. The accelerated durability tests (ADTs) were used to evaluate the durability of catalysts, which adopted 30000 cyclic voltammetry loops between 0.6- 1.1 V (vs. RHE) with a sweep rate of 100 mV s⁻¹ in a 0.1M O₂-saturated HClO₄ solution.

4. Membrane electrode assemblies (MEAs) tests:

The MEAs device combined with the machine of Arbin to test performance of catalysts in the practical application potential in PEMFCs. Firstly, 68.4 mg of catalysts were mixture with 5 wt.% Nafion (342.1 mg), deionized water (1026.3 mg) and isopropyl alcohol (1026.3 mg) with ultrasonic dispersion for 3 h. The ink was sprayed to a 15 mm thick gore film (effective load area is 6.25 cm²) by a spray gun, in which cathode supported Pt1Fe1-IMC/C catalyst or JM-20% Pt/C catalyst with the loading of 0.2 mg cm⁻² and anode supported JM-60% Pt/C catalyst with the loading of 0.1 mg cm⁻².

The steady-state polarization curve of MEAs were employed to investigate the practical application potential of catalyst in PEMFC under H₂/Air (back pressure:1bar / 2bar) or H₂/O₂ (back pressure:1bar) at 80 °C. In addition, discharging under constant current density of 1 A cm⁻² (100 h) was carried out to evaluate the stability under the same condition.

Results and Discussion

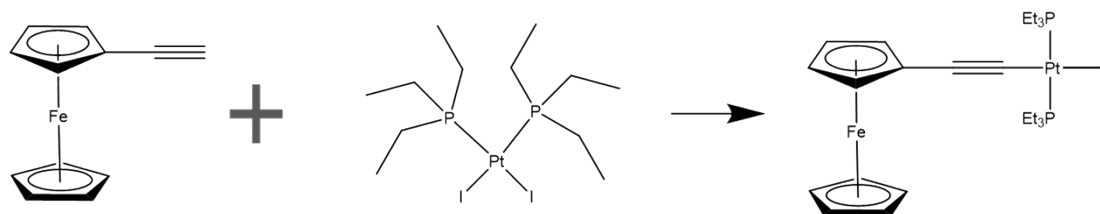


Figure S1. Chemical reaction equations for synthesis of HBOM.

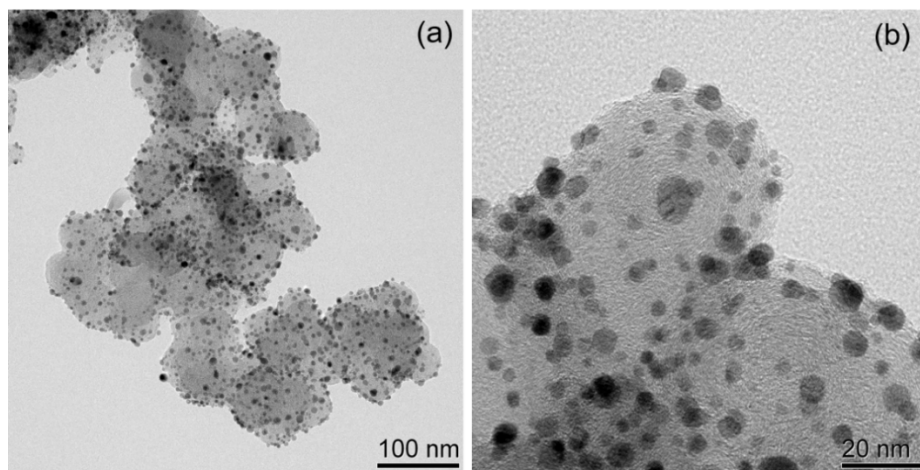


Figure S2. (a), (b) TEM images for the prepared Pt1Fe1-IMC catalyst.

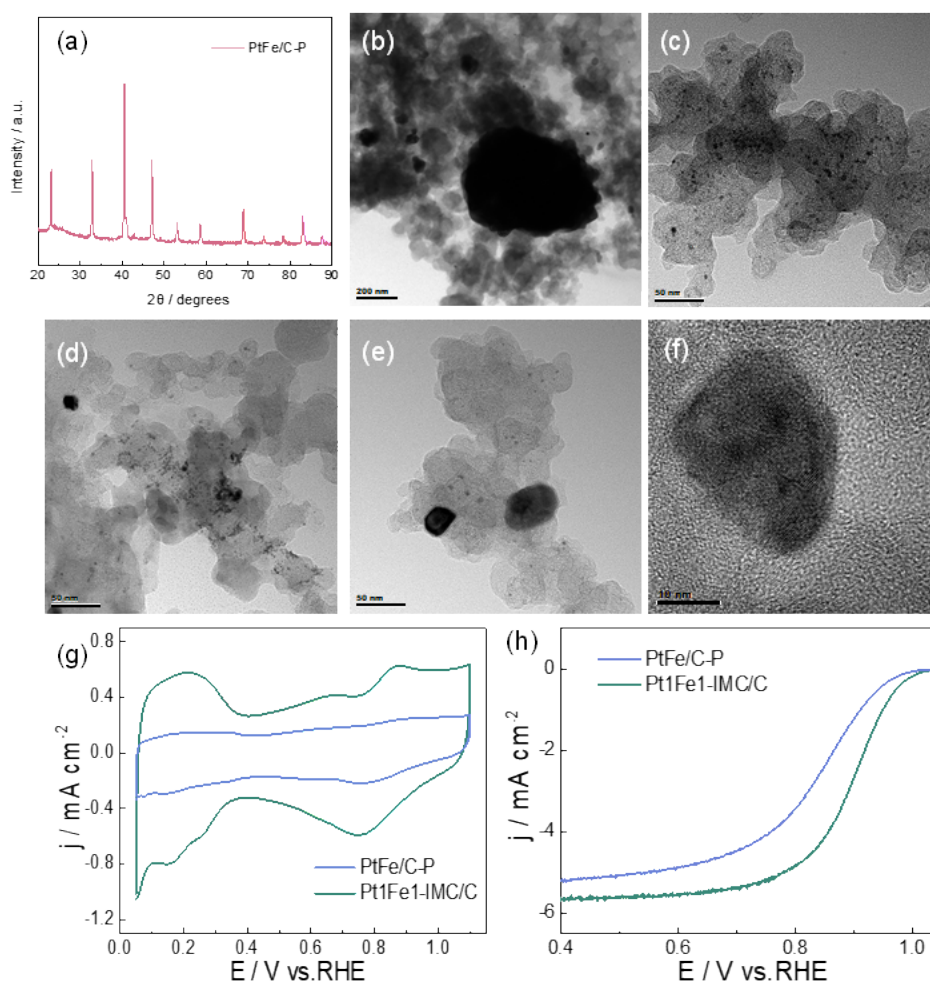


Figure S3. (a) XRD pattern, and (b) ~ (f) TEM images for the prepared PtFe/C-P sample; (g), (h) CV and LSV curves for PtFe/C-P and Pt1Fe1-IMC/C.

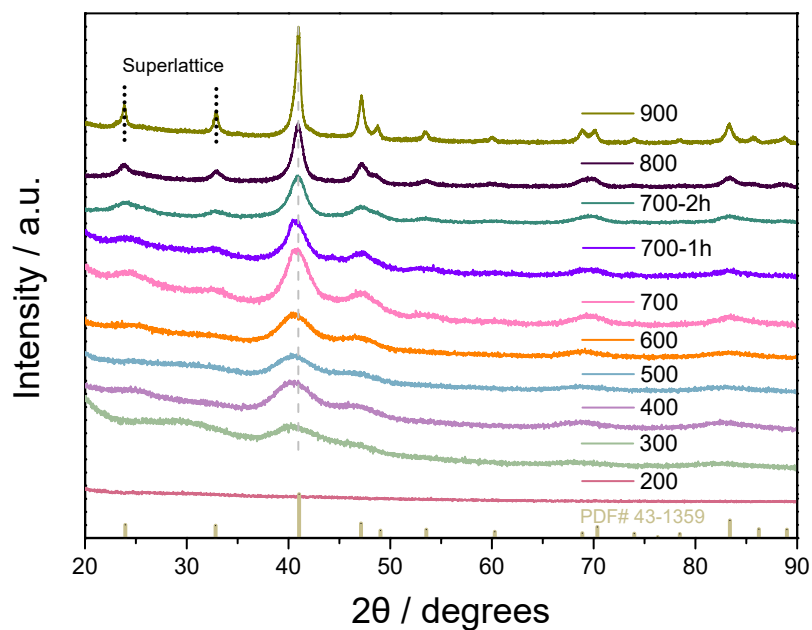


Figure S4. Temperature/time-dependent ex-situ XRD patterns of Pt1Fe1-IMC/C catalyst during the annealing process.

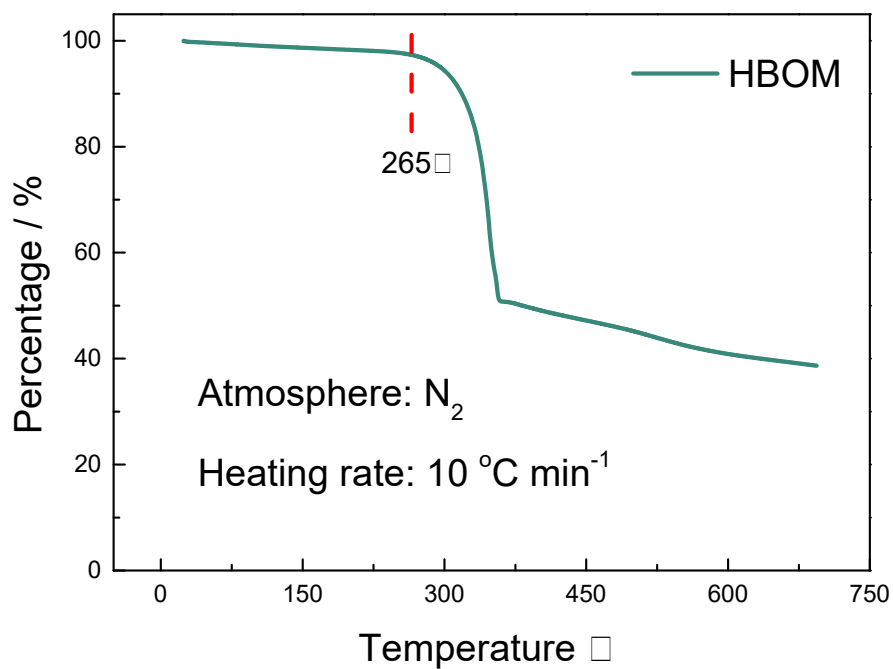


Figure S5. TG curve for the HBOM.

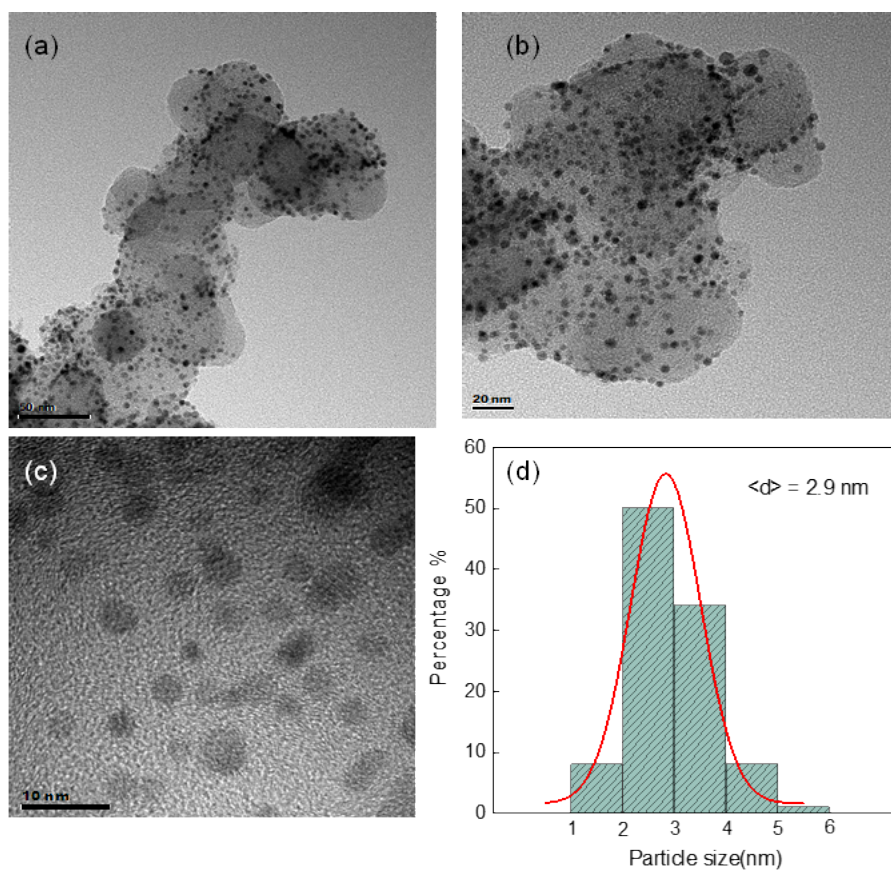


Figure S6. (a)~(c) TEM images and (d) size distribution histogram for D-PtFe/C.

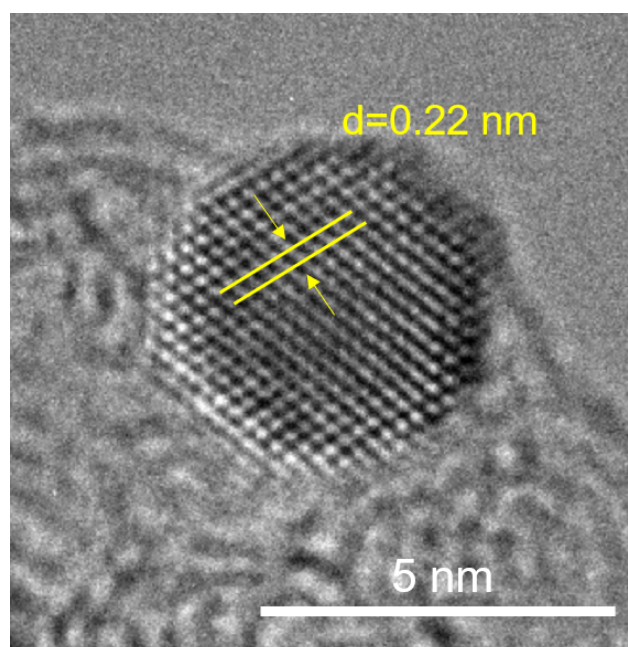


Figure S7. High-resolution TEM image for Pt₁Fe₁-IMC/C catalyst.

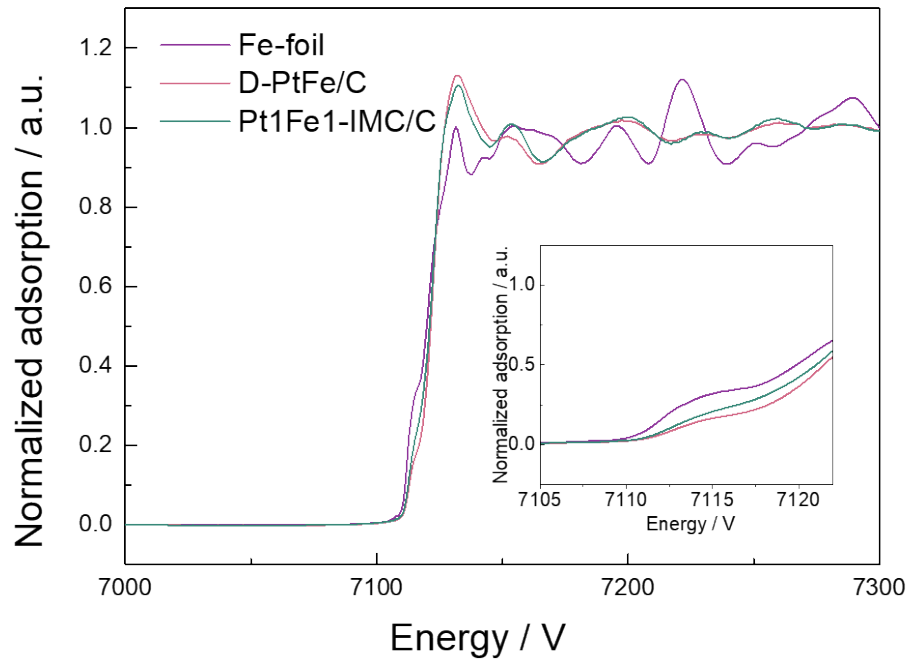


Figure S8. XANES of Fe for Fe foil, D-PtFe/C and Pt1Fe1-IMC/C.

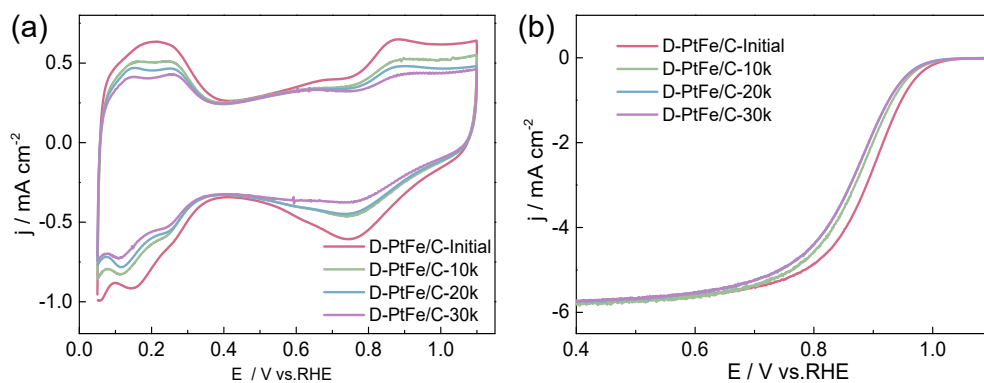


Figure S9. (a), (b) CV and LSV curves before and after ADT for D-PtFe/C.

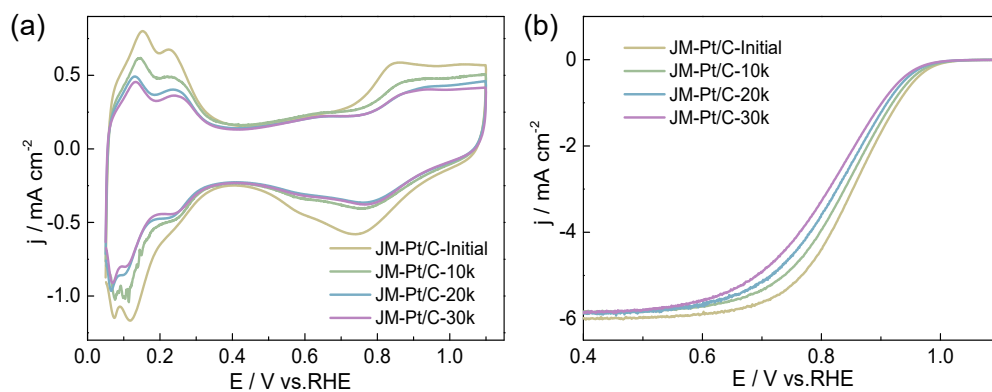


Figure S10. (a), (b) CV and LSV curves before and after ADT for JM-Pt/C.

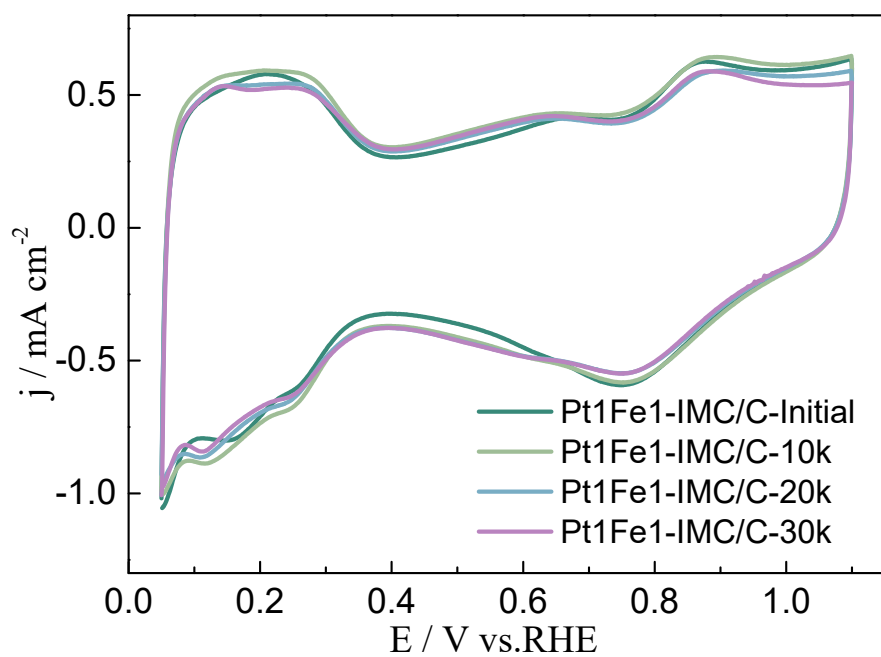


Figure S11. CV curves before and after ADT for Pt1Fe1-IMC/C.

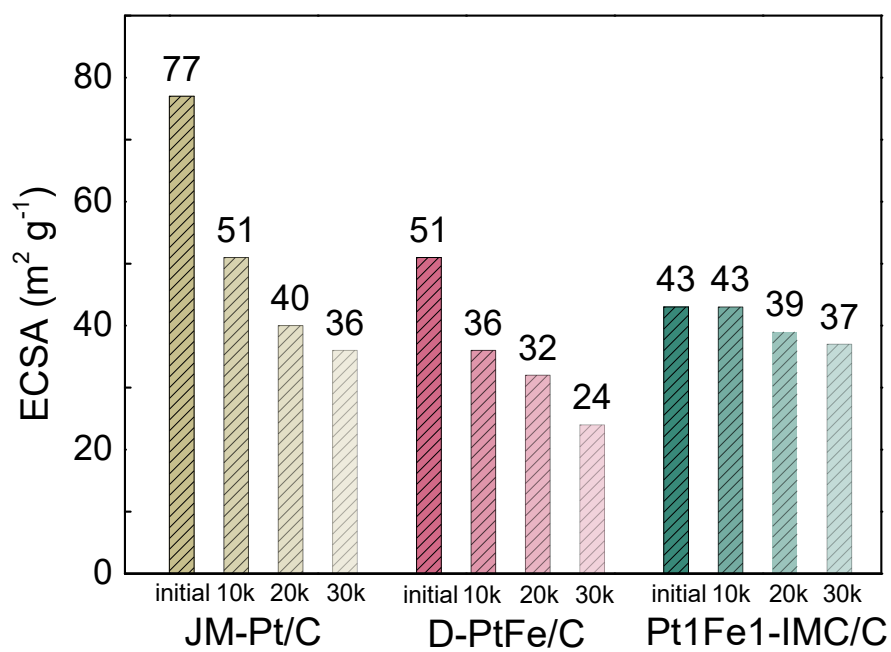


Figure S12. ECSA before and after ADT for Pt1Fe1-IMC/C, D-PtFe/C and JM-Pt/C.

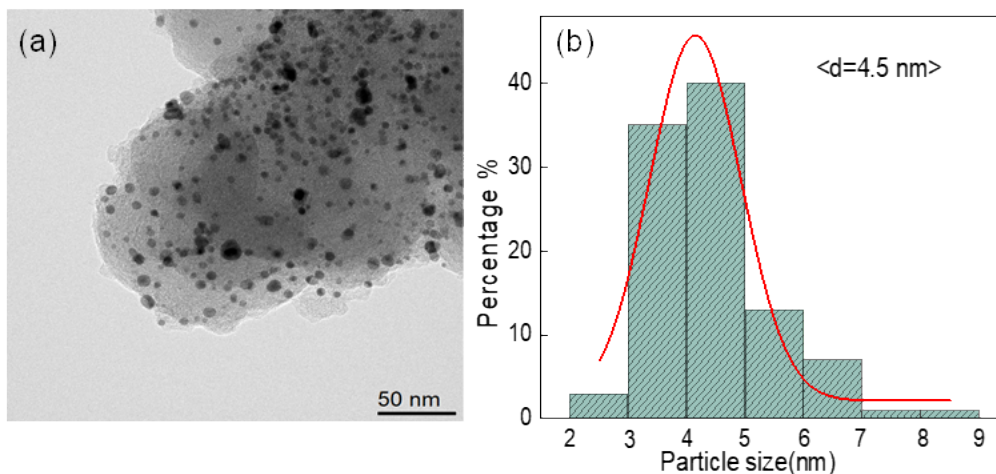


Figure S13. (a) TEM images and (b) size distribution histogram for Pt1Fe1-IMC/C after 30k ADT.

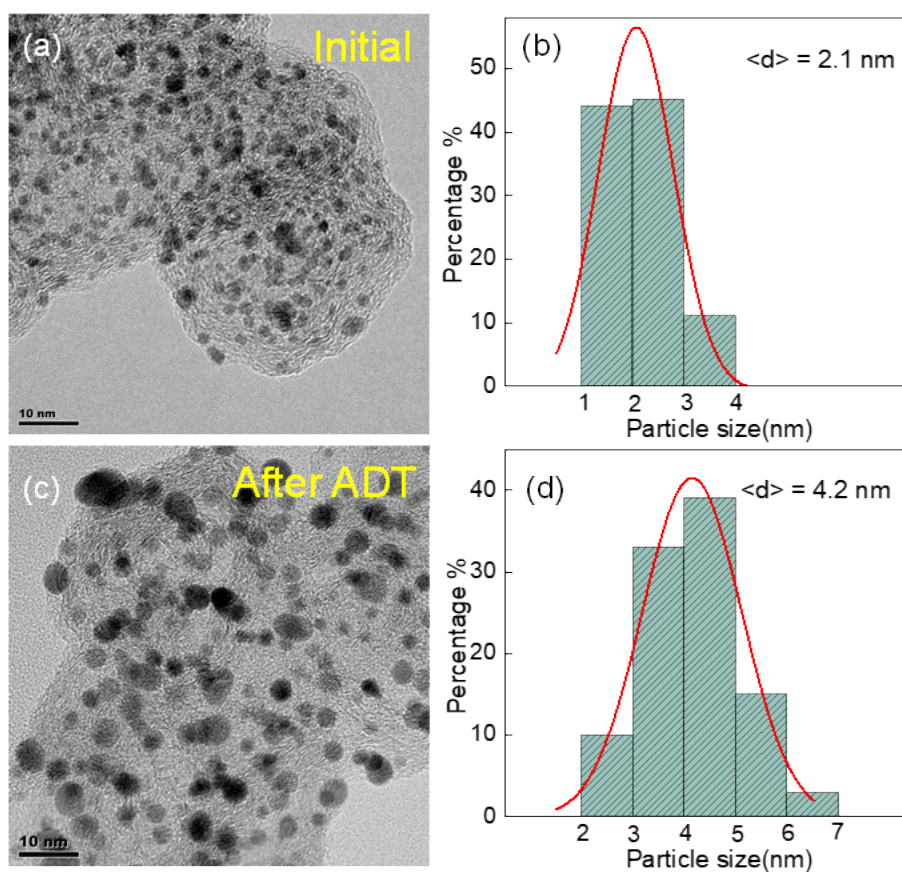


Figure S14. TEM images and size distribution histogram for JM-Pt/C before (a), (b) and after (c) (d) ADT.

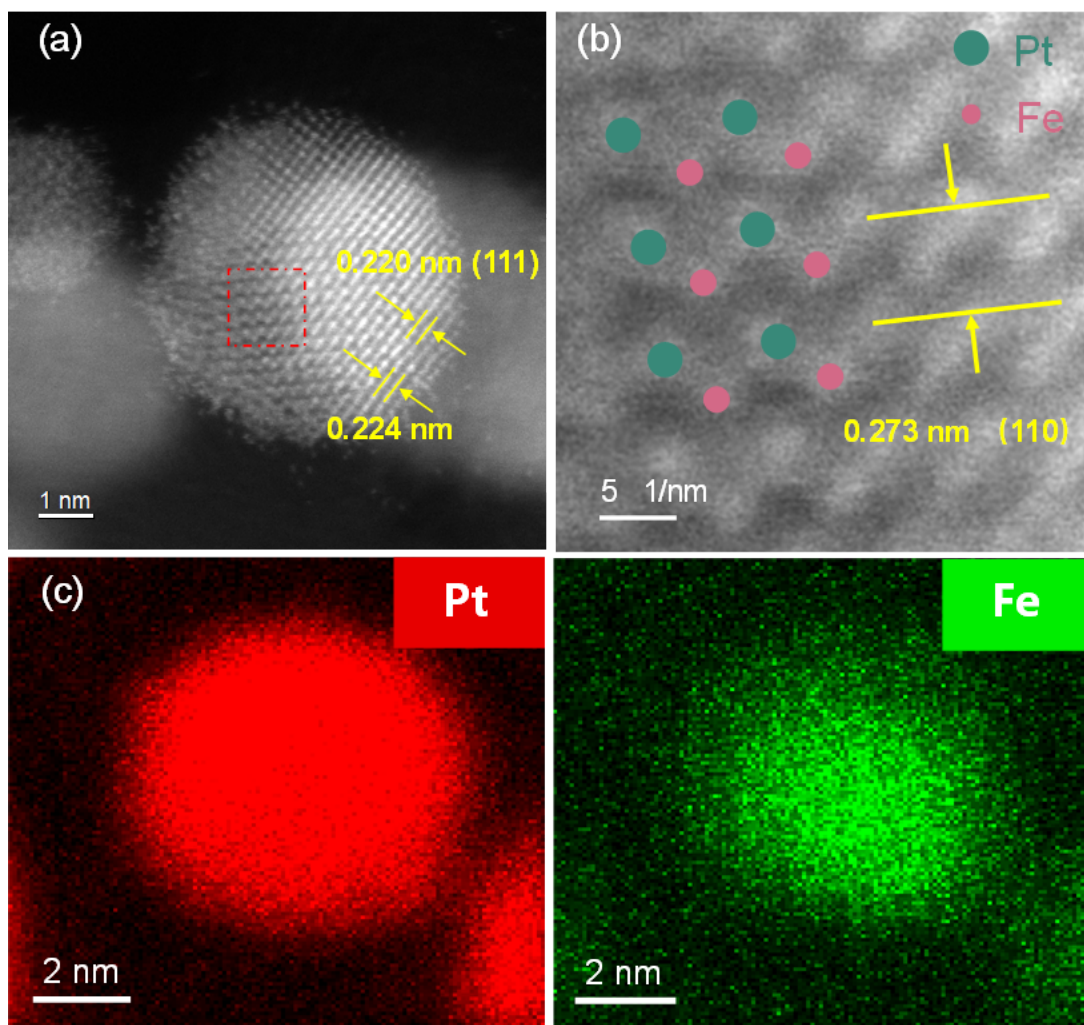


Figure S15. (a) Atomic-resolution STEM and (b) enlarged image (c) EDS-mapping for Pt₁Fe₁-IMC/C after 30k ADT.

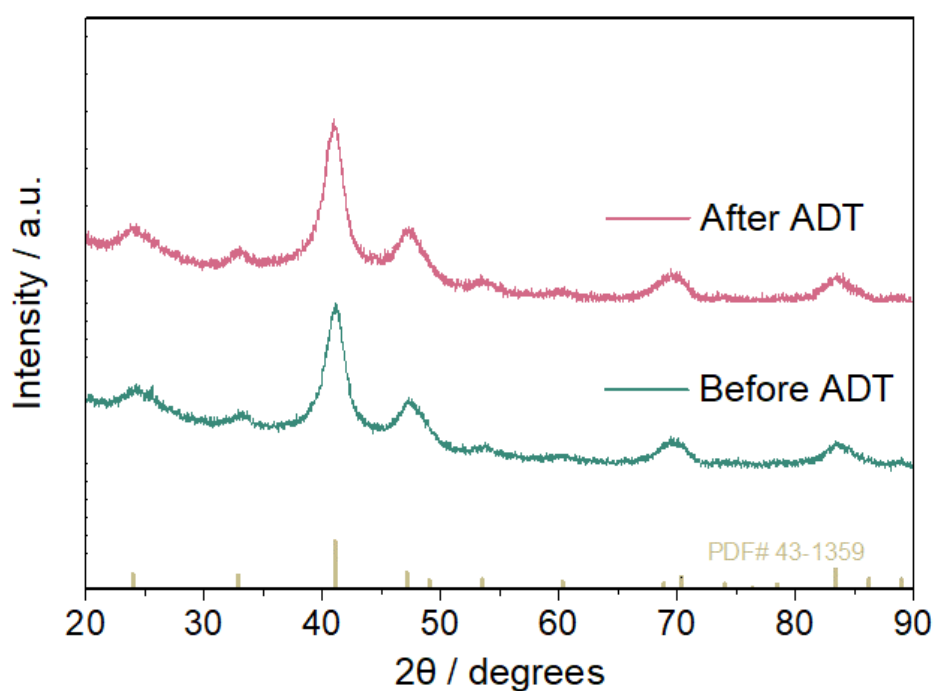


Figure S16. XRD patterns for Pt1Fe1-IMC/C before and after 30k ADT.

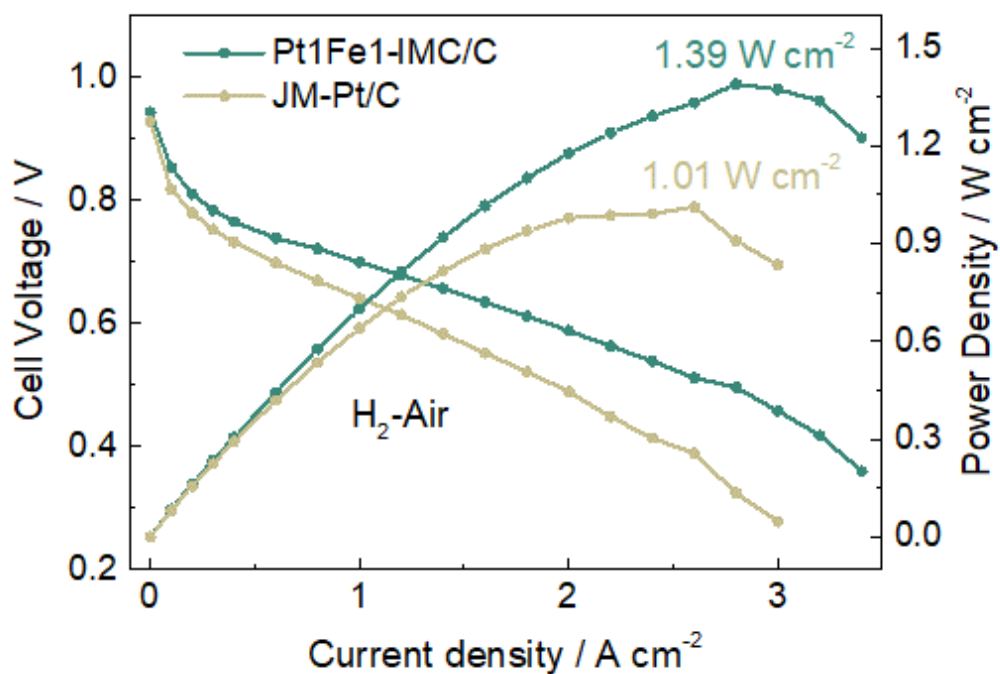


Figure S17. Steady-state polarization curves of MEAs with Pt1Fe1-IMC/C and JM-Pt/C as the cathode under H₂-Air conditions. The test conditions of MEA include 2 bar back pressure, 80 °C, 100%RH; Anode: 0.1 mg_(Pt) cm⁻², 1 slpm, 1.2 (stoichiometric); Cathode: 0.2 mg_(Pt) cm⁻², 1.5 slpm, 1.5 (stoichiometric).

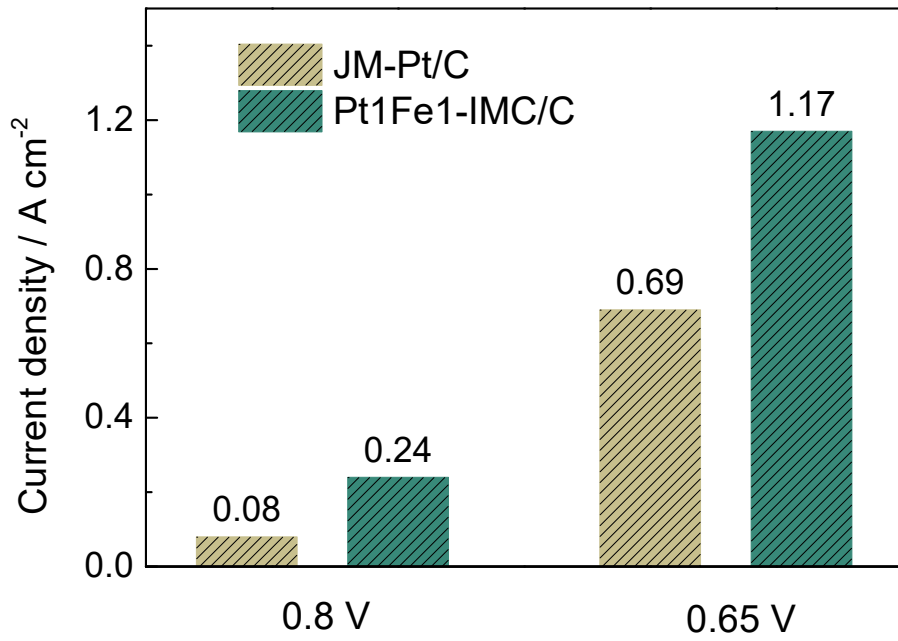


Figure S18. Current densities for Pt1Fe1-IMC /C and JM-Pt/C at 0.8 and 0.65 V in the MEA test.

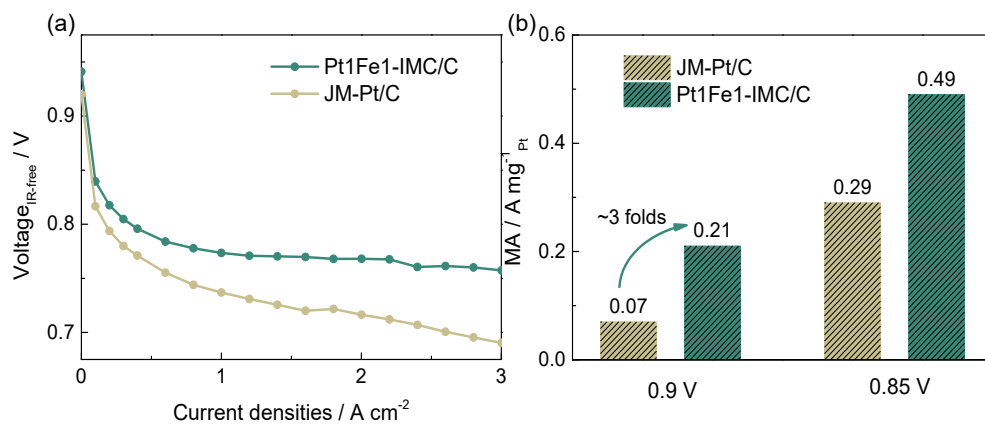


Figure S19. (a) IR-free polarization curves for Pt1Fe1-IMC/C and JM-Pt/C catalysts under H₂-O₂ condition; (b) mass activities for Pt1Fe1-IMC/C and JM-Pt/C at 0.9 and 0.85 V in the MEA test.

Table S1. EDS for HBOM at various locations.

| EDS site | Atomic Pt:Fe |
|----------|--------------|
| #1 | 52.80: 47.20 |
| #2 | 53.07: 46.93 |
| #3 | 49.03:50.97 |

Table S2. The performance of advanced Pt-based catalysts as cathode in PEMFCs under H₂-air/ H₂-O₂ conditions.

| Sample | Power density / mWcm ⁻² (H ₂ -air) | Power density / mWcm ⁻² (H ₂ -O ₂) | Reference |
|-------------------|---|--|-----------|
| Pt1Fe1-IMC/C | 1.21 (Cathode :0.2 mgcm ⁻² BP ^[a] :100 kPa, 80 °C, 100% RH) | 2.47 (Cathode: 0.2 mgcm ⁻² BP:100 kPa, 80 °C, 100%RH) | This work |
| LP@PF-2 | ~0.80 (Cathode: 0.043 mgcm ⁻² BP: 100 kPa, 80 °C, 100% RH) | 1.42 (Cathode: 0.043 mgcm ⁻² BP: 100 kPa, 80 °C, 100% RH) | 2 |
| PtCo/NGC | 0.697 (Cathode: 0.1 mgcm ⁻² BP: 170 kPa, 80 °C, 60% RH) | \ | 3 |
| PtNi alloy | 0.92 (Cathode: 0.15 mgcm ⁻² BP: 200 kPa, 80 °C, 100% RH) | \ | 4 |
| Coplanar Pt/C | 0.553 (Cathode: 0.1 mgcm ⁻² BP: 150 kPa, 80 °C, 100% RH) | 0.91 (Cathode: 0.1 mgcm ⁻² BP: 100kPa, 80 °C, 100%RH) | 5 |
| P-Pt/C | 1.06 (Cathode: 0.15 mgcm ⁻² BP: 50 kPa, 80 °C, 100% RH) | ~1.25 (Cathode: 0.15 mgcm ⁻² BP: 50kPa, 80 °C, 100%RH) | 6 |
| Ga-PtNi/C | 0.42 (Cathode: 0.15 mgcm ⁻² BP: 1 atom, 65 °C, 100% RH) | \ | 7 |
| Dealloyed PtNi | ~0.9 (Cathode: 0.1 mgcm ⁻² BP: 150 kPa, 80 °C, 100% RH) | \ | 8 |
| Pt67Co31W2 | ~0.6 (Cathode: 0.11 mgcm ⁻² BP: 150 kPa, 80 °C, 100% RH) | \ | 9 |
| Dealloyed PtNi/C | ~0.82 (Cathode: 0.1 mgcm ⁻² BP: 100kPa, 80 °C, 100% RH) | \ | 10 |
| Pt/40Co-NC-900 | ~0.7 (Cathode:0.13 mgcm ⁻² BP: 150kPa, 80 °C, 100% RH) | \ | 11 |
| Pt1Co1-IMC@Pt/C | 1.13 (Cathode: 0.1 mgcm ⁻² BP: 100kPa, 80 °C, 100% RH) | 2.3 (Cathode: 0.2 mgcm ⁻² BP: 100 kPa, 80 °C, 100% RH) | 12 |
| Fine grain PtFe/C | ~0.59 (Cathode: 0.225 mgcm ⁻² BP: 150kPa, 80 °C, 100% RH) | \ | 13 |

[a] BP: back pressure

Table S3. Ordering degree for catalysts in Figure S4

| Name | Ordering degree |
|--------|-----------------|
| 700 | 69% |
| 700-1h | 73% |
| 700-2h | 78% |
| 800 | 81% |
| 900 | 75% |

References

1. F. Sembera, J. Plutnar, A. Higelin, Z. Janousek, I. Cisarova and J. Michl, *Inorg. Chem.*, 2016, **55**, 3797-3806.
2. L. Chong, J. Wen, J. Kubal, F. G. Sen, J. Zou, J. Greeley, M. Chan, H. Barkholtz, W. Ding and D. J. Liu, *Science*, 2018, **362**, 1276-1281.
3. W. S. Jung, W. H. Lee, H.-S. Oh and B. N. Popov, *J. Mater. Chem. A*, 2020, **8**, 19833-19842.
4. X. Tian, X. Zhao, Y. Q. Su, L. Wang, H. Wang, D. Dang, B. Chi, H. Liu, E. J.M. Hensen, X. W. Lou and B. Y. Xia, *Science*, 2019, **366**.
5. Y. Hu, M. Zhu, X. Luo, G. Wu, T. Chao, Y. Qu, F. Zhou, R. Sun, X. Han, H. Li, B. Jiang, Y. Wu and X. Hong, *Angew. Chem. Int. Ed.*, 2021, **60**, 6533-6538.
6. B. A. Lu, L. F. Shen, J. Liu, Q. Zhang, L. Y. Wan, D. J. Morris, R. X. Wang, Z. Y. Zhou, G. Li, T. Sheng, L. Gu, P. Zhang, N. Tian and S. G. Sun, *ACS Catal.*, 2020, **11**, 355-363.
7. J. Lim, H. Shin, M. Kim, H. Lee, K. S. Lee, Y. Kwon, D. Song, S. Oh, H. Kim and E. Cho, *Nano. Lett.*, 2018, **18**, 2450-2458.
8. B. Han, C. E. Carlton, A. Kongkanand, R. S. Kukreja, B. R. Theobald, L. Gan, R. O'Malley, P. Strasser, F. T. Wagner and Y. Shao-Horn, *Energy Environ. Sci.*, 2015, **8**, 258-266.
9. J. Liang, N. Li, Z. Zhao, L. Ma, X. Wang, S. Li, X. Liu, T. Wang, Y. Du, G. Lu, J. Han, Y. Huang, D. Su and Q. Li, *Angew. Chem. Int. Ed.*, 2019, **58**, 15471-15477.
10. F. Dionigi, C. C. Weber, M. Primbs, M. Gocyla, A. M. Bonastre, C. Spori, H. Schmies, E. Hornberger, S. Kuhl, J. Drnec, M. Heggen, J. Sharman, R. E. Dunin-Borkowski and P. Strasser, *Nano. Lett.*, 2019, **19**, 6876-6885.
11. X. X. Wang, S. Hwang, Y. T. Pan, K. Chen, Y. He, S. Karakalos, H. Zhang, J. S. Spendelow, D. Su and G. Wu, *Nano. Lett.*, 2018, **18**, 4163-4171.
12. Q. Cheng, S. Yang, C. Fu, L. Zou, Z. Zou, Z. Jiang, J. Zhang and H. Yang, *Energy Environ. Sci.*, 2022, **15**, 278-286.
13. X. X. Du, Y. He, X. X. Wang and J. N. Wang, *Energy Environ. Sci.*, 2016, **9**, 2623-2632.

Author Contributions

DeChaoLai: Conceptualization, Methodology, Validation, Writing – original draft; Qingqing Cheng: Conceptualization, Methodology, Writing; Yu Zheng: Formal analysis, Methodology; Hao Zhao: Investigation, Data curation; Yunbin Chen: Investigation, Formal analysis; Weibo Hu: Investigation; Liangliang Zou: Investigation, Resources; Zhiqing Zou: Investigation; Ke Wen: Investigation; Hui Yang: Validation, Data curation, Supervision, Resources.